Enhanced Interleukin (IL)-13 Responses in Mice Lacking IL-13 Receptor α 2

Nancy Wood,[1] Matthew J. Whitters,[2] Bruce A. Jacobson,[1] JoAnn Witek,[2] Joseph P. Sypek,[1] Marion Kasaian,[1] Michael J. Eppihimer,[1] Michelle Unger,[1] Takashi Tanaka,[3] Samuel J. Goldman,[1] Mary Collins,[2] Debra D. Donaldson,[1] and Michael J. Grusby[3]

[1]*Department of Respiratory Disease and* [2]*Department of Musculoskeletal Sciences, Wyeth Research, Cambridge, MA 02140*

[3]*Department of Immunology and Infectious Diseases, Harvard School of Public Health, Boston, MA 02115*

The Journal of Experimental Medicine

Abstract

Interleukin (IL)-13 has recently been shown to play important and unique roles in asthma, parasite immunity, and tumor recurrence. At least two distinct receptor components, IL-4 receptor (R)α and IL-13Rα1, mediate the diverse actions of IL-13. We have recently described an additional high affinity receptor for IL-13, IL-13Rα2, whose function in IL-13 signaling is unknown. To better appreciate the functional importance of IL-13Rα2, mice deficient in IL-13Rα2 were generated by gene targeting. Serum immunoglobulin E levels were increased in IL-13Rα2$^{-/-}$ mice despite the fact that serum IL-13 was absent and immune interferon γ production increased compared with wild-type mice. IL-13Rα2–deficient mice display increased bone marrow macrophage progenitor frequency and decreased tissue macrophage nitric oxide and IL-12 production in response to lipopolysaccharide. These results are consistent with a phenotype of enhanced IL-13 responsiveness and demonstrate a role for endogenous IL-13 and IL-13Rα2 in regulating immune responses in wild-type mice.

Key words: receptors • immunoglobulin E • interleukin 13 • knockout mice • nitric oxide

Introduction

Expression of Th2 cytokines such as IL-4, IL-5, IL-9, and IL-13, and inflammation are strongly associated with parasitic infections and asthma (1, 2). For this reason, significant effort has been focused on understanding the contribution of individual Th2 cytokines and their receptors to disease progression in animal models. Within this family of cytokines, IL-13 has recently been shown to play a necessary role in protective immunity against nematodes and a detrimental role in immune responses associated with schistosomiasis and asthma (3–6).

Receptor binding chains for IL-13 include IL-13Rα1 and IL-13Rα2 (7–10). IL-13Rα1 binds IL-13 with low affinity. Coexpression of IL-13Rα1 with IL-4Rα results in the formation of a high affinity receptor signaling complex (8, 9, 11). This receptor complex is widely expressed on both lymphoid and nonlymphoid cells and can also be activated by IL-4, thus accounting for the significant overlap in IL-4 and IL-13 activities (12). In contrast to IL-13Rα1, IL-13Rα2 selectively binds IL-13 with high affinity and its contribution to IL-13 signaling is unknown. The cytoplasmic region of murine IL-13Rα2 does not posses an obvious signaling motif or Janus kinase/signal transducer and activator of transcription (STAT)* binding sequence (10). Expression of IL-13Rα2 transcripts are restricted to spleen and brain and in contrast to IL-13Rα1, a soluble form of this receptor has been detected in mouse serum (13). Similar to the IL-1 type II receptor (14), IL-13Rα2 may function as a decoy to attenuate IL-13 effects in vivo.

IL-13 has been shown to have many different activities on numerous cell types. In vitro studies of antigen-presenting cells have demonstrated that IL-13 generally inhibits activation-induced cytokine and nitric oxide (NO) production from macrophages (15–17) and increases IgE pro-

Address correspondence to Debra D. Donaldson, Wyeth Research, 200 CambridgePark Drive, Cambridge, MA 02140. Phone: 617-665-5549; Fax: 617-665-5584; E-mail: ddonaldson@wyeth.com

**Abbreviations used in this paper:* EMSA, electrophoretic mobility shift assay; MLF, murine lung fibroblasts; NO, nitric oxide; RPA, RNase protection assay; RPM, resident peritoneal macrophages; STAT, signal transducer and activator of transcription.

 J. Exp. Med. © The Rockefeller University Press • 0022-1007/2003/03/703/7 $8.00
Volume 197, Number 6, March 17, 2003 703–709
http://www.jem.org/cgi/doi/10.1084/jem.20020906

duction from human B cells (18). In addition, administration of rIL-13 in vivo or transgenic overexpression of IL-13 leads to the enhancement of both macrophage development and IgE production and affords protection to LPS-induced endotoxemia (4, 19–23).

To understand the role of IL-13Rα2 in regulating the biologic responses to IL-13, we examined the effect of a targeted deletion of IL-13Rα2. IL-13Rα2–deficient mice display enhanced macrophage development and IgE production consistent with the notion that IL-13Rα2 can serve to limit IL-13 responses in vivo.

Materials and Methods

Animals. A gene targeting vector was designed such that homologous recombination would delete the translation initiation site and signal peptide of the endogenous gene encoding IL-13Rα2. Male *IL-13Rα2*$^{-/-}$ mice were generated from (129 × C57BL/6) mice and were backcrossed onto the BALB/c strain. BALB/c littermates at the identical stage of backcrossing between 8–14 wk of age were used within each experiment. Littermates after three to four generations were used in histopathology studies and biochemical studies (see Fig. 2). Littermates after 8–10 generations were used in functional assays (see Figs. 3–5). Animals were maintained under pathogen-free conditions in accordance with guidelines from the Committee on Animals of the Harvard Medical School and Wyeth Research, National Research Council, and the American Association for the Accreditation of Laboratory Animal Care.

Western Blotting. Pooled sera was diluted with one volume of cell lysis buffer (Tris buffered saline: 20 mM Tris, 150 mM NaCl, pH 7.5; 1% Triton X-100, 40 mg iodoacetamide per 25 ml, and 1 tablet of protease inhibitor cocktail; Boehringer). Three to five million cells were lysed in 1.5 ml lysis buffer. IL-13Rα2 was precipitated with 2.5 μg biotinylated Chinese hamster ovary murine IL-13 (4) and streptavidin agarose beads (Pierce Chemical Co.). After washing, samples were subjected to 12% SDS-PAGE and transferred to polyvinylidene difluoride (NEN Life Science Products) by semidry electroblotting. The blot was incubated with polyclonal rabbit sera to murine IL-13Rα2 (5 μg/ml; 24). Peroxidase-labeled goat anti–rabbit IgG (1:20,000; Jackson ImmunoResearch Laboratories) was added as a second step. The blot was developed with enhanced chemiluminescence reagents and exposed on Hyperfilm (Amersham Biosciences).

Electrophoretic Mobility Shift Assay (EMSA). Cells were cultured on 60 × 15–mm plates in complete media until 85% confluent. Cells were washed twice with RPMI and incubated in RPMI for 1.5 h before stimulation with cytokines. Cytokines were added for 15 min and the adherent murine lung fibroblasts (MLF) were harvested with trypsin and washed once with ice-cold PBS. The cells were lysed in 3 packed volumes with lysis buffer (20 mM Hepes-HCl, 20% glycerol, 500 mM KCl, 0.5 mM DTT, 1 mM sodium orthovanadate, 5 mM sodium fluoride, 0.2 mM EDTA, 0.1% Triton X-100, and one-half protease inhibitor tablet; Boehringer). The protein concentration from the whole cell extract was determined by micro bicinchonic acid (Pierce Chemical Co.). 10 μm protein was mixed with 4 μg poly dI-dC (Amersham Biosciences), 5× gel shift buffer (20 mM Hepes, pH 7.9, 50 mM KCl, 10% glycerol, 0.5 mM DTT, and 0.1 mMEDTA), and anti-STAT1 or anti-STAT6 (Santa Cruz Biotechnology, Inc.) Ab in a total volume of 14 μl. The mixture was incubated for 2 h at 4°C. The STAT6-specific radiolabeled probe (25,000 cpm in 1 μl; reference 25) was added for 20 min at 30°C. The samples were electrophoresed on a 5% polyacrylamide gel in 0.5× Tris-glycine buffer. The gel was dried before film exposure.

RNase Protection Assay (RPA). MLF were grown in medium with or without murine IL-4 or murine IL-13 (R&D Systems) at 10 ng/ml. RNA was isolated at 4 and 24 h using the QIAGEN RNeasy mini purification kit. Two micrograms RNA per sample were used for analysis of receptor expression in the mCR-1 RiboQuant Multiprobe RPA (BD Biosciences). Note that the technical data sheet for mCR-1 assigns the name IL-13Rα2 to the template derived from IL-13Rα1. To study IL-13Rα2 in this system we generated a 206-bp template (including 32 bp vector sequence) in vitro by inserting bases 973–1129 of IL-13LRα2 (sequence data available from GenBank/EMBL/DDBJ under accession no. NM_008356) into pGEM-3Zf(−) (Promega). ^{32}P-labeled antisense probe was synthesized by T7 RNA polymerase from IL-13Rα2 template in combination with the mCR-1 template. The 172-bp protected probe for IL-13α2 was easily resolved from IL-2Rα (190 bp) and L32 (141 bp) probes on denaturing polyacrylamide gels followed by autoradiography at −70°C overnight.

Culture of Ba/F3, Ba/F3.IL-13Rα2, Ba/F3.IL-13Rα1, IL-13Rα2$^{-/-}$ *MLF, and IL-13Rα2*$^{+/+}$ *MLF.* Culture of Ba/F3 lines has been described (10). MLF were isolated from lung explants and enriched by repeated passage in vitro. In brief, the lung was harvested, minced, and incubated in trypsin solution for 1 h at 37°C. The MLF were cultured on human collagen–coated plastic at 12.5 μg/ml (Biomedical Technologies Inc.) in MEM containing 20% FBS, 1% MEM vitamins, 1% MEM nonessential amino acids, 1% antibiotic/antimycotic (GIBCO BRL), 10 U/ml heparin, 154 μg/ml endothelial mitogen (BTI), and 5 × 10^{-5} M 2-ME. MLF were used at passage 15.

Peritoneal Cell Preparation and Stimulation In Vitro. Resident peritoneal cells were harvested by peritoneal lavage using 7 ml cold PBS. Cell concentration was adjusted such that 5 × 10^4 CD11b$^+$ (BD Biosciences) macrophages were adhered per well in a 96-well plate. After a 2-h incubation at 37°C, 5% CO_2, the nonadherent cells were removed by rinsing several times with RPMI without serum. Macrophages were then cultured in serum-free RPMI supplemented with antibiotics, 10^{-2} M morpholinopropane sulfonic acid (buffer), 5 × 10^{-5} M 2-ME, 2.5 mg/ml BSA, 10 μg/ml transferrin, and 1 μU/ml insulin (GIBCO BRL).

Measurement of NO and Cytokine Production. Macrophages (prepared as described above) were cultured with 20 ng/ml IFN-γ (R&D Systems) and 20 ng/ml LPS (Sigma-Aldrich). Supernatants were harvested after 48 h. Nitrite, as an indicator of NO production, was determined spectrophotometrically by using the standard Griess reaction with sodium nitrite used as a standard. In brief, 50 μl supernatant was mixed with 50 μl of 1% sulfanilamide and 50 μl of 0.1% napthylethylenediamine dihydrochloride. Absorbence was measured at 550 nm using an automated plate reader. Cytokines were measured by ELISA (R&D Systems). IL-13 was used at concentrations noted in the figures. Cells were treated with IL-13 for 16–20 h before the addition of IFN-γ and LPS.

Cytokine Production Assays. Spleens were harvested aseptically and single cell suspensions were prepared and erythrocytes were lysed using ammonium chloride. 2 ml cells at a concentration of 4 × 10^6 cells/ml in RPMI containing 100 U penicillin/ml, 100 μg streptomycin/ml, 2 mM glutamine, 5 × 10^{-5} M 2-ME, and 10% FCS were plated in 24-well tissue culture plates (Costar).

Cells were incubated alone or stimulated with 0.1 ug/ml anti-CD3 (BD Biosciences) or 1 ug/ml LPS. Supernatants were collected at 72 h and stored at −20°C until analyzed. Cytokines were measured by ELISA (R&D Systems).

Ig Subclass ELISAs. ELISA plates (MaxiSorp; Nunc) were coated overnight at 4°C with goat anti–mouse κ light chain (Sigma-Aldrich) for IgM, IgA, and IgG3 assays, goat anti–mouse IgG, Fab specific (Sigma-Aldrich) for IgG2a and IgG1, goat anti–mouse IgG, Fc specific (Sigma-Aldrich) for IgG2b, and rat anti–mouse IgE (BD Biosciences) for IgE. All incubations were performed for 1–2 h at room temperature. Plates were blocked with 0.5% gelatin in PBS, washed in PBS containing 0.05% Tween-20 (PBS-Tween), and incubated with purified mouse Igs (BD Biosciences) as standards or with serum dilutions. Specificity was achieved with the appropriate biotinylated antibodies to IgM, IgA, IgG2a, IgG2b, IgG3 (Southern Biotechnology Associates, Inc.), IgG1, or IgE (BD Biosciences) and use of mouse IgG or IgM antibodies (Sigma-Aldrich) for blocking. Binding was detected with peroxidase-linked streptavidin (Southern Biotechnology Associates, Inc.) and tetramethylbenzidine substrate (Kirkegaard and Perry Labs.).

Serum IL-13 ELISA. Mouse IL-13 ELISA kits were purchased from R&D Systems. Assays were performed according to the manufacturer's instructions, with the exception that 100 μg/ml rabbit IgG anti–IL-13Rα2 Ab (24) was added during the primary incubation period to a 1:10 or 1:100 dilution of serum samples and incubated overnight at 4°C to dissociate IL-13 from serum IL-13Rα2. Duplicate serum samples were examined from each animal. OD readings were converted to pg/ml using a standard curve and the appropriate dilution factor.

Preparation of Tissue Extracts. Excised lung and liver were weighed, homogenized, and freeze/thawed as previously described except that a Brinkmann homogenizer was used (26). Homogenates were centrifuged in a microfuge at 4°C and the supernatants were used for the measurement of cytokines.

MethoCult Colony Assay. Bone marrow was obtained from the femurs of three *IL-13Rα2*$^{-/-}$ and *IL-13Rα2*$^{+/+}$ mice. Bone marrow cells were washed twice with DME plus 10% FCS and counted in methylene blue. Cells were plated at 10^5 cells/ml in MethoCult complete media containing 1% BSA and growth factors (insulin, transferrin, IL-3, IL-6, stem cell factor, and erythropoietin; StemCell Technologies Inc.) in triplicate in 12-well cluster dishes at 1 ml/well. Cultures were grown for 6 d and colonies were counted through an inverted phase contrast microscope. Colonies were differentiated based on phenotype: large uniformly red colonies, burst forming unit erythroid; mixed colonies including granuloctye, erythrocyte, macrophage, and megakaryocyte; and large, diffuse colonies composed of only macrophages.

Statistical Analysis. Significance was assessed with Student's unpaired, two-tailed *t* test. P values <0.05 were considered to be significant.

Results

Generation of IL-13Rα2$^{-/-}$ *Mice.* *IL-13Rα2*$^{-/-}$ mice were viable, fertile, and displayed no overt abnormalities in appearance, weight, nor behavior. Examination of serum from *IL-13Rα2*$^{-/-}$ mice failed to reveal soluble IL-13Rα2 capable of binding IL-13 demonstrating that the mice lack IL-13Rα2 (Fig. 1). Detailed necropsy including histopathology, serum chemistry, and hematology did not reveal any obvious abnormalities. FACS® analysis of cell suspensions from lymphoid and hematopoietic tissues of wild-type mice failed to show differences in cell number nor expression levels for: CD3, CD90, CD45, CD69, CD4, and CD8 on thymocytes; CD45, B220, CD23, CD11b, CD11c, CD3, CD4, CD8, and class I and II on splenocytes; CD45, Gr-1, Ter-119, CD11b, and B220 on bone marrow cells; CD3, CD5, CD8, B220, CD4, CD19, CD23, and CD11b on peripheral blood cells; and CD16/32, CD14, CD5, CD19, CD3, and class I and II on peritoneal cells.

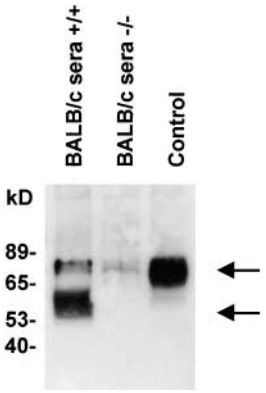

Figure 1. Generation of *IL-13Rα2*$^{-/-}$ mice. Analysis of IL-13Rα2 expression from serum. Sera was pooled from four *IL-13Rα2*$^{-/-}$ and four *IL-13Rα2*$^{+/+}$ male mice. IL-13Rα2 was precipitated and detected by western with rabbit polyclonal antisera to recombinant IL-13Rα2. Lysed Ba/F3.IL-13Rα2 (reference 10) cells were used as a positive control. The bottom arrow indicates murine IL-13Rα2 precipitated from the sera of *IL-13Rα2*$^{+/+}$ but not *IL-13Rα2*$^{-/-}$ mice. The top arrow identifies IL-13Rα2 precipitated from Ba/F3.IL-13Rα2 lysate. The nonspecific band at 65 kD was also present in parental Ba/F3 cells (unpublished data).

STAT6 Signaling Is Preserved in Fibroblasts from IL-13Rα2$^{-/-}$ *Mice.* IL-13 activates STAT6 in fibroblasts (27) and fibroblasts play an important role in chronic immune responses. Therefore, we examined the expression of IL-13R components in MLF from wild-type mice. Passage 15 MLF were stimulated with IL-13 or IL-4 and examined for receptor expression using RPA. Fig. 2 A shows that MLF express IL-13Rα1 and IL-4Rα transcripts without stimulation and IL-13Rα2 within 4 (unpublished data) or 24 h after the addition of IL-13 or IL-4. Low levels of IL-13Rα2 transcripts are detected at early passages in MLF culture by RPA without stimulation (unpublished data). Fig. 2 B shows that MLF derived from *IL-13Rα2*$^{-/-}$ and *IL-13Rα2*$^{+/+}$ mice exposed to IL-13 display STAT6 activation as measured by EMSA assay. Complementing the results of Kawakami et al. (28) and Murata et al. (11), these results show that in MLF, IL-13Rα2 is not required for IL-13–induced STAT6 activation.

Serum, Tissue, and Immune Activation Levels of IL-13 in IL-13Rα2$^{+/+}$ *and IL-13Rα2*$^{-/-}$ *Mice.* We have previously demonstrated the presence of IL-13 in wild-type and parasite-infected mouse serum using a modified ELISA (24). The ELISA specifically minimizes the quenching effect of IL-13Rα2 and measures total IL-13 in wild-type serum. To study the effect of IL-13Rα2 deficiency on serum IL-13 levels we measured the levels of IL-13 in the serum in *IL-13Rα2*$^{-/-}$ and *IL-13Rα2*$^{+/+}$ mice. Fig. 3 A shows that *IL-13Rα2*$^{-/-}$ mice had greatly reduced or undetectable levels of serum IL-13 compared to *IL-13Rα2*$^{+/+}$ mice, which had average serum levels of 90 pg/ml. To ascertain that the loss of IL-13 expression in the serum was not due to lack of IL-13 production in *IL-13Rα2*$^{-/-}$ mice, we evaluated the results of polyclonal stimulation of spleen

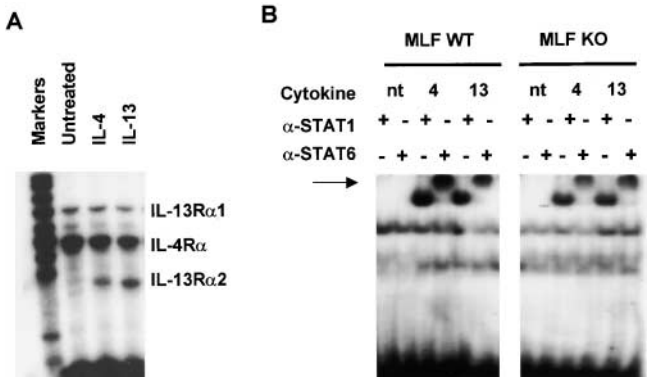

Figure 2. STAT6 signaling is preserved in *IL-13Rα2*$^{-/-}$ mice in response to IL-13 in fibroblasts that express IL-13 receptor transcripts. (A) IL-13 receptor transcripts are expressed by MLF. RPA was performed with total RNA from passage 15 MLF untreated or treated for 24 h with IL-4 or IL-13. Transcripts are identified according to molecular weight of free probe in marker lane. (B) STAT6 signaling is intact in lung fibroblasts from *IL-13Rα2*$^{-/-}$ mice. MLF from *IL-13Rα2*$^{+/+}$ and *IL-13Rα2*$^{-/-}$ mice respond to IL-13 with STAT6 activation as shown by EMSA. Fibroblasts grown from the lung of *IL-13Rα2*$^{+/+}$ and *IL-13Rα2*$^{-/-}$ mice were stimulated with 100 ng/ml IL-4 or 100 ng/ml IL-13 for 15 min. Cytoplasmic extracts and ^{32}P-labeled probe were incubated with or without anti-STAT1 or anti-STAT6. In the presence of anti-STAT6 the complex migration is retarded (arrow) compared with samples without Ab.

cells with CD3 or LPS. Fig. 3 B shows that anti-CD3–stimulated spleen cells from *IL-13Rα2*$^{-/-}$ mice produce IL-13 at a level only slightly lower than *IL-13Rα2*$^{+/+}$ mice. Matsukawa et al. (26) previously demonstrated the presence of IL-13 in tissue extract from the liver and lung. Using their extraction method we compared the levels of lung and liver IL-13 in *IL-13Rα2*$^{-/-}$ and *IL-13Rα2*$^{+/+}$ mice and found that levels of tissue IL-13 are significantly elevated in *IL-13Rα2*$^{-/-}$ mice compared with *IL-13Rα2*$^{+/+}$ mice (Fig. 3 C). Taken together, these results suggest that the presence of IL-13Rα2 is required to regulate the levels of serum and tissue IL-13.

Serum IgE, IgA, IgG2a, and IgG2b, and Immune-dependent IFN-γ Production Are Elevated in IL-13Rα2$^{-/-}$ *Mice.* IgE levels are increased in both IL-4–deficient IL-13 transgenic mice and in IL-4–deficient mice infected with malaria (23, 29). Similarly, an increased level of serum IgE is observed in mice after the administration of IL-13 (4). Therefore, we wished to study the effect of IL-13Rα2 deficiency on serum Ig isotype levels. Fig. 4 A shows that serum IgA, IgE and IgG2a, and IgG2b are significantly elevated in *IL-13Rα2*$^{-/-}$ mice. IL-13 has been shown to affect the function of accessory cells such as B cells (30) and macrophages (15), and IL-13 deficiency has been shown to impair Th2 differentiation (31). In contrast, IL-13 has not been demonstrated to function directly on T cells. Therefore, we examined cytokine production from spleen cells in response to activation with anti-CD3 in *IL-13Rα2*$^{+/+}$ and *IL-13Rα2*$^{-/-}$ mice. Fig. 4 B shows that the level of IFN-γ is increased nearly twofold in spleen cultures from *IL-13Rα2*$^{-/-}$ mice whereas IL-13 (Fig. 3 C) levels are only slightly decreased and IL-10 levels slightly increased. Taken together, these results suggest that IL-13Rα2 serves to attenuate levels of IFN-γ and the downstream Ig serum isotypes that are regulated by IFN-γ and IL-13.

Bone Marrow Macrophage Progenitors Are Increased from IL-13Rα2$^{-/-}$ *Mice.* IL-13 and parasite-treated mice display peripheral monocytosis and extramedullary hematopoiesis (19). To determine if IL-13Rα2 plays a role in bone marrow macrophage development we determined the frequency of hematopoietic cell progenitors in bone marrow methylcellulose cultures. As shown in Fig. 5 A, *IL-13Rα2*$^{-/-}$ mice had significantly higher frequencies of bone marrow macrophage progenitors per femur as demonstrated by increased macrophage colony formation. In addition, frequencies of immature erythroid (as measured by burst forming unit erythroid) progenitors per femur were significantly reduced. However, examination of immature bone marrow erythroid precursor (TER-119) frequency, splenic colony formation and peripheral blood lymphocyte populations failed to show differences (unpublished data). These results are similar to that seen when IL-13 is administered to mice (19) and are consistent with enhanced IL-13 activity in the absence of IL-13Rα2.

Peritoneal Macrophages from IL-13Rα2$^{-/-}$ *Mice Release Less NO and IL-12 in Response to LPS than IL-13Rα2*$^{+/+}$ *Mice.* To address the hypothesis that deficiency of IL-13Rα2 might affect mature macrophage function, we compared the ability of *IL-13Rα2*$^{+/+}$ and *IL-13Rα2*$^{-/-}$ resident peritoneal macrophages (RPM) to generate NO in response to IFN-γ and LPS. Pretreatment of mouse bone

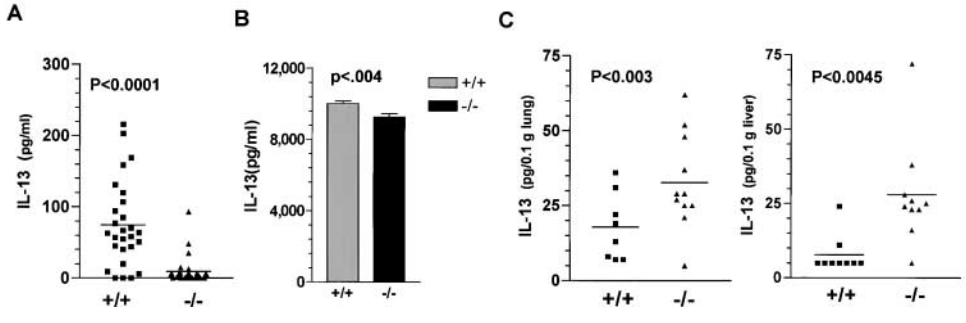

Figure 3. Tissue and immune but not serum IL-13 expression is preserved in *IL-13Rα2*$^{-/-}$ mice. Sera (A) and lung and liver tissue homogenates (C) from 8–20 individual *IL-13Rα2*$^{-/-}$ and *IL-13Rα2*$^{+/+}$ mice were assayed by ELISA for IL-13. (B) 4 × 10^6/ml spleen cells pooled from four to five mice were pooled and incubated with 0.1 ug/ml anti-CD3. 72 h after stimulation, cell supernatants from triplicate wells were harvested and assayed by ELISA for IL-13. Data are representative of at least three experiments, multiple groups with five mice per group, and are given as mean values ± SEM. P values for significant difference between groups as determined by Student's unpaired, two-tailed *t* test are noted.

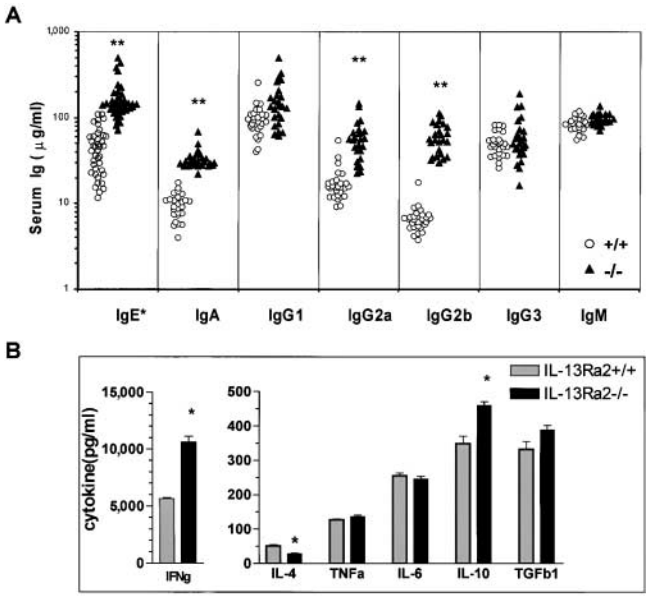

Figure 4. Serum IgE, IgA, IgG2a, and IgG2b, and immune-dependent IFN-γ production are elevated in *IL-13Rα2*$^{-/-}$ mice. (A) Analysis of wild-type serum Ig isotypes. Sera from 24–32 individual animals were analyzed. Data represent mean of triplicate wells. **, $P < 0.0001$ for IgE, IgA, Ig2a, and Ig2b. (B) Cytokine production from anti-CD3–activated spleen cells. 4×10^6/ml spleen cells pooled from four to five mice and incubated with 0.1 ug/ml anti-CD3. 72 h after stimulation, cell supernatants from triplicate wells were harvested and assayed by ELISA for cytokines. Data are representative of at least three experiments, multiple groups with five mice per group, and are given as mean values ± SEM. *, significant difference between groups as determined by Student's unpaired, two-tailed *t* test; *, $P < 0.0001$.

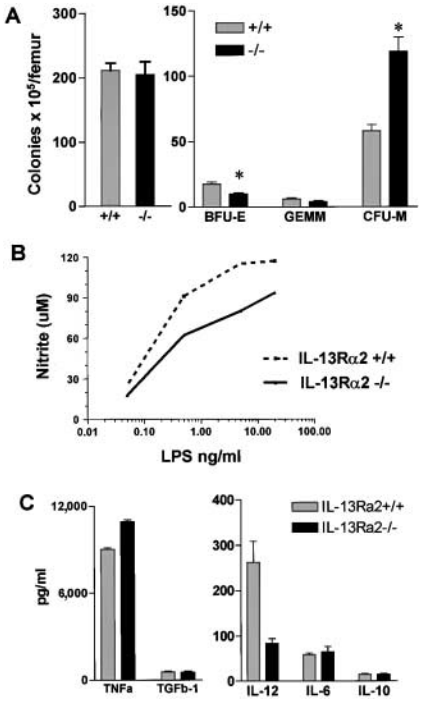

Figure 5. Tissue macrophage progenitors are increased in *IL-13Rα2*$^{-/-}$ mice and produce less NO in response to LPS. (A) Bone marrow macrophage progenitors are increased in *IL-13Rα2*$^{-/-}$ mice. Bone marrow from three *IL-13Rα2*$^{-/-}$ and *IL-13Rα2*$^{+/+}$ mice was harvested and cultured separately as described in Materials and Methods. Colony morphology and frequency were determined using an inverted microscope. Data represent three mice per group and are given as mean values ± SEM. *$P < 0.05$, significant difference between groups as determined by Student's unpaired, two-tailed *t* test. (B) Activation-induced tissue macrophage NO is attenuated in *IL-13Rα2*$^{-/-}$ mice. Levels of macrophage NO detected after 48 h from pooled cultures of four to five mice stimulated with increasing concentration of LPS and constant level of IFN-γ at 20 ng/ml. Data are representative of at least five experiments. (C) Activation-induced IL-12 but not TNF-α, TGF-β, IL-10, nor IL-6 is attenuated in *IL-13Rα2*$^{-/-}$ mice. Level of IL-12 detected after 48 h by macrophages stimulated with increasing concentration of LPS and constant level of IFN-γ at 20 ng/ml. Data are representative of at least five experiments.

marrow macrophages or peritoneal macrophages with IL-13 or IL-4 has been shown to suppress IFN-γ–induced NO production in a STAT6-dependent fashion (15, 32, 33). Consistent with preserved STAT6 activation in fibroblasts, we observed that pretreatment of RPM from *IL-13Rα2*$^{+/+}$ and *IL-13Rα2*$^{-/-}$ mice resulted in a depression of NO (unpublished data). Fig. 5 B shows that NO production is less in *IL-13Rα2*$^{-/-}$ RPM compared with *13Rα2*$^{+/+}$ RPM after combined IFN-γ and LPS activation. Higher doses of LPS are required to induce NO in *IL-13Rα2*$^{-/-}$ mice demonstrating that macrophages from *IL-13Rα2*$^{-/-}$ mice are less sensitive to LPS than *IL-13Rα2*$^{+/+}$ mice.

IL-13 treatment of macrophages in vitro before or coincident with exposure to LPS has been shown to modulate production of proinflammatory cytokines such at IL-6, TNF, and IL-12, and the antiinflammatory cytokine IL-10 (15–17). However, the consequence of IL-13 treatment in these investigations varies depending on the nature and culture conditions of the macrophages being studied. In contrast, systemic administration of IL-13 before exposure to LPS in vivo has consistently been shown to protect mice from endotoxemia and is associated with decreased TNF, IFN-γ, IL-12, and IL-10 production (20–22). Consistent with these results, we also observed that pretreatment of RPM from *IL-13Rα2*$^{+/+}$ and *IL-13Rα2*$^{-/-}$ mice resulted in a depression of LPS-induced TNF production (unpublished data). Therefore, we wished to study the effect of LPS on cytokine production from *IL-13Rα2*$^{+/+}$ and *IL-13Rα2*$^{-/-}$ RPM. Fig. 5 C shows that IL-12 production is decreased in *IL-13Rα2*$^{-/-}$ RPM. IL-10 and TGF-β are not changed in *IL-13Rα2*$^{-/-}$ RPM. TNF-α levels from *IL-13Rα2*$^{-/-}$ RPM were variable and slightly increased as shown in this experiment and slightly decreased in other experiments.

Discussion

In this report we describe the generation of mice deficient in IL-13Rα2 to define the role of this receptor chain in IL-13 responses. IL-13Rα2 may act to modulate the effects of IL-13 in vivo in various ways. IL-13Rα2 could enhance IL-13 activities by increasing the strength of IL-13

signaling or attenuate IL-13 effects by negative signaling or simply as a molecular decoy. Attenuating roles of IL-13Rα2 could explain the lack of evidence for IL-13 effects on T cells or an enhancing role could explain the effect of IL-13 effect on airways hyperreactivity and eosinophil survival distinct from IL-4.

Interestingly, we find that the absence of IL-13Rα2 correlates with nearly complete loss of serum IL-13 and an increase in tissue IL-13 in *IL-13Rα2*$^{-/-}$ mice. The lack of serum IL-13 cannot be explained by a lack of IL-13 production in *IL-13Rα2*$^{-/-}$ mice as IL-13 is present in tissues of *IL-13Rα2*$^{-/-}$ and is produced by activated *IL-13Rα2*$^{-/-}$ immune cells. Serum IL-13Rα2 may act as a reservoir for serum IL-13 and extend IL-13 half-life or may function as a natural antagonist of IL-13 as has been shown for IL-4 receptor (34, 35). We have previously shown that the administration of IL-13Rα2.Fc is effective as an antagonist of IL-13 in vivo (6, 36). In addition, increased tissue IL-13 in *IL-13Rα2*$^{-/-}$ mice cannot be explained by slightly decreased levels of immune IL-13 production. This suggests that in the liver and lung, IL-13Rα2 acts to decrease tissue cytokine levels, possibly via equilibrium with the serum reservoir. Finally, IL-13 appears to regulate the expression of IL-13Rα2, suggesting that ligand and receptor may cross regulate one another.

We find that serum IgE, IgG2a, IgG2b, and IgA levels are increased in *IL-13Rα2*$^{-/-}$ mice. Lai and Mosmann (30) have shown that the administration of IL-13 in vivo enhances plasma levels of IgG2a and IgG2b and B cell survival in vitro. Concurrent changes in IgE may not have been detected in their studies due to assay sensitivity (30). Increased serum IgE independent of IL-4 was demonstrated in transgenic mice overexpressing IL-13 (23). Conversely, Bost et al. (37) have shown that mice treated with anti–IL-13 during oral immunization have significantly reduced intestinal IgA, serum IgA, and serum IgG. Taken together, these data suggest that IL-13 can enhance IgE, IgG2a, IgG2b, and IgA levels in vivo and are consistent with an enhanced IL-13 response in IL-13Rα2–deficient mice.

Here, we show that *IL-13Rα2*$^{-/-}$ mice have increased macrophage progenitors and decreased tissue macrophage NO and IL-12 production. This is similar to previous studies showing that IL-13 administration in vivo affects monocyte/macrophage development and reduces the sensitivity of mice to LPS-induced shock (20–22). In addition, the decreased responsiveness of immune cells to LPS in *IL-13Rα2*$^{-/-}$ mice, as shown by decreased expression of IL-12, is similar to studies in vivo showing a diminished response to LPS after the administration of IL-13 (20). Levels of IL-10, TGF-β, and prostaglandin E2 (unpublished data), and IL-4 production are similar from *IL-13Rα2*$^{+/+}$– and *IL-13Rα2*$^{-/-}$–derived macrophages and spleen cells and cannot explain the decreased production of NO in response to LPS and IFN-γ.

Taken together, our studies indicate that overall IL-13Rα2 serves to dampen IL-13–mediated responses in vivo. The absence of this receptor results in decreased responsiveness to LPS, increased levels of bone marrow macrophage progenitors, and enhanced levels of serum IgA, IgE, IgG2a, and IgG2b in wild-type mice. All of these effects are consistent with enhanced IL-13 responses in vivo. This interpretation is also consistent with the enhancement of IL-13–mediated fibrosis observed in *Schistosoma mansoni*–infected *IL-13Rα2*$^{-/-}$ mice (38). These studies serve to underscore the potent role IL-13 plays in both wild-type mice and in mice undergoing vigorous immune responses to pathogens and the necessity for precise control of IL-13 levels in vivo.

The authors thank Bijia Deng for Ig ELISAs, members of the Wynn lab for advice and useful discussions, Ed Clark, Jim Calvetti, and JoAnn Yetz-Aldape for expert technical assistance, and Page Bouchard for evaluation of histology.

M.J. Grusby is supported by National Institutes of Health grants AI4040171 and GM62135, and awards from the Sandler Family Supporting Foundation and the Mathers Foundation.

Submitted: 4 June 2002
Revised: 23 January 2003
Accepted: 23 January 2003

References

1. Wills-Karp, M. 1999. Immunologic basis of antigen-induced airway hyperresponsiveness. *Annu. Rev. Immunol.* 17:255–281.
2. Finkelman, F.D., T.A. Wynn, D.D. Donaldson, and J.F. Urban. 1999. The role of IL-13 in helminth-induced inflammation and protective immunity against nematode infections. *Curr. Opin. Immunol.* 11:420–426.
3. Urban, J.F., Jr., N. Noben-Trauth, D.D. Donaldson, K.B. Madden, S.C. Morris, M. Collins, and F.D. Finkelman. 1998. IL-13, IL-4Ralpha, and Stat6 are required for the expulsion of the gastrointestinal nematode parasite Nippostrongylus brasiliensis. *Immunity*. 8:255–264.
4. Wills-Karp, M., J. Luyimbazi, X. Xu, B. Schofield, T.Y. Neben, C.L. Karp, and D.D. Donaldson. 1998. Interleukin-13: central mediator of allergic asthma. *Science*. 282:2258–2261.
5. Grunig, G., M. Warnock, A.E. Wakil, R. Venkayya, F. Brombacher, D.M. Rennick, D. Sheppard, M. Mohrs, D.D. Donaldson, R.M. Locksley, et al. 1998. Requirement for IL-13 independently of IL-4 in experimental asthma. *Science*. 282:2261–2263.
6. Chiaramonte, M.G., L.R. Schopf, T.Y. Neben, A.W. Cheever, D.D. Donaldson, and T.A. Wynn. 1999. IL-13 is a key regulatory cytokine for Th2 cell-mediated pulmonary granuloma formation and IgE responses induced by Schistosoma mansoni eggs. *J. Immunol.* 162:920–930.
7. Caput, D., P. Laurent, M. Kaghad, J.M. Lelias, S. Lefort, N. Vita, and P. Ferrara. 1996. Cloning and characterization of a specific interleukin (IL)-13 binding protein structurally related to the IL-5 receptor alpha chain. *J. Biol. Chem.* 271: 16921–16926.
8. Aman, M.J., N. Tayebi, N.I. Obiri, R.K. Puri, W.S. Modi, and W.J. Leonard. 1996. cDNA cloning and characterization of the human interleukin 13 receptor alpha chain. *J. Biol. Chem.* 271:29265–29270.
9. Hilton, D.J., J.G. Zhang, D. Metcalf, W.S. Alexander, N.A. Nicola, and T.A. Willson. 1996. Cloning and characterization of a binding subunit of the interleukin 13 receptor that is

also a component of the interleukin 4 receptor. *Proc. Natl. Acad. Sci. USA.* 93:497–501.
10. Donaldson, D., M. Whitters, L. Fitz, T. Neben, H. Finnerty, S. Henderson, R.M. O'Hara, Jr., D. Beier, K. Turner, C. Wood, et al. 1998. The murine IL-13 receptor α2: molecular cloning, characterization, and comparison with murine IL-13 receptor α1. *J. Immunol.* 161:2317–2324.
11. Murata, T., J. Taguchi, and R.K. Puri. 1998. Interleukin-13 receptor alpha′ but not alpha chain: a functional component of interleukin-4 receptors. *Blood.* 91:3884–3891.
12. Zurawski, S.M., F. Vega, Jr., B. Huyghe, and G. Zurawski. 1993. Receptors for interleukin-13 and interleukin-4 are complex and share a novel component that functions in signal transduction. *EMBO J.* 12:2663–2670.
13. Zhang, J.G., D.J. Hilton, T.A. Willson, C. McFarlane, B.A. Roberts, R.L. Moritz, R.J. Simpson, W.S. Alexander, D. Metcalf, and N.A. Nicola. 1997. Identification, purification, and characterization of a soluble interleukin (IL)-13-binding protein. Evidence that it is distinct from the cloned Il-13 receptor and Il-4 receptor alpha-chains. *J. Biol. Chem.* 272: 9474–9480.
14. Colotta, F., S. Orlando, E.J. Fadlon, S. Sozzani, C. Matteucci, and A. Mantovani. 1995. Chemoattractants induce rapid release of the interleukin 1 type II decoy receptor in human polymorphonuclear cells. *J. Exp. Med.* 181:2181–2186.
15. Doherty, T.M., R. Kastelein, S. Menon, S. Andrade, and R.L. Coffman. 1993. Modulation of murine macrophage function by IL-13. *J. Immunol.* 151:7151–7160.
16. Bogdan, C., H. Thuring, M. Dlaska, M. Rollinghoff, and G. Weiss. 1997. Mechanism of suppression of macrophage nitric oxide release by IL-13: influence of the macrophage population. *J. Immunol.* 159:4506–4513.
17. Doyle, A.G., G. Herbein, L.J. Montaner, A.J. Minty, D. Caput, P. Ferrara, and S. Gordon. 1994. Interleukin-13 alters the activation state of murine macrophages in vitro: comparison with interleukin-4 and interferon-gamma. *Eur. J. Immunol.* 24:1441–1445.
18. Punnonen, J., G. Aversa, B.G. Cocks, A.N. McKenzie, S. Menon, G. Zurawski, R. de Waal Malefyt, and J.E. de Vries. 1993. Interleukin 13 induces interleukin 4-independent IgG4 and IgE synthesis and CD23 expression by human B cells. *Proc. Natl. Acad. Sci. USA.* 90:3730–3734.
19. Lai, Y.H., J.M. Heslan, S. Poppema, J.F. Elliot, and T.R. Mosmann. 1996. Continuous administration of IL-13 to mice induces extramedullary hemopoiesis and monocytosis. *J. Immunol.* 156:3166–3173.
20. Muchamuel, T., S. Menon, P. Pisacane, M.C. Howard, and D.A. Cockayne. 1997. IL-13 protects mice from lipopolysaccharide-induced lethal endotoxemia: correlation with down-modulation of TNF-alpha, IFN-gamma, and IL-12 production. *J. Immunol.* 158:2898–2903.
21. Nicoletti, F., G. Mancuso, V. Cusumano, R. Di Marco, P. Zaccone, K. Bendtzen, and G. Teti. 1997. Prevention of endotoxin-induced lethality in neonatal mice by interleukin-13. *Eur. J. Immunol.* 27:1580–1583.
22. Di Santo, E., C. Meazza, M. Sironi, P. Fruscella, A. Mantovani, J.D. Sipe, and P. Ghezzi. 1997. IL-13 inhibits TNF production but potentiates that of IL-6 in vivo and ex vivo in mice. *J. Immunol.* 159:379–382.
23. Emson, C.L., S.E. Bell, A. Jones, W. Wisden, and A.N. McKenzie. 1998. Interleukin (IL)-4–independent induction of immunoglobulin (Ig)E, and perturbation of T cell development in transgenic mice expressing IL-13. *J. Exp. Med.* 188:399–404.
24. Finkelman, F.D., S.C. Morris, T. Orekhova, M. Mori, D. Donaldson, S.L. Reiner, N.L. Reilly, L. Schopf, and J.F. Urban, Jr. 2000. Stat6 regulation of in vivo IL-4 responses. *J. Immunol.* 164:2303–2310.
25. Schindler, U., P. Wu, M. Rothe, M. Brasseur, and S.L. McKnight. 1995. Components of a Stat recognition code: evidence for two layers of molecular selectivity. *Immunity.* 2:689–697.
26. Matsukawa, A., C.M. Hogaboam, N.W. Lukacs, P.M. Lincoln, H.L. Evanoff, R.M. Strieter, and S.L. Kunkel. 2000. Expression and contribution of endogenous IL-13 in an experimental model of sepsis. *J. Immunol.* 164:2738–2744.
27. Haque, S.J., P. Harbor, M. Tabrizi, T. Yi, and B.R. Williams. 1998. Protein-tyrosine phosphatase Shp-1 is a negative regulator of IL-4- and IL-13-dependent signal transduction. *J. Biol. Chem.* 273:33893–33896.
28. Kawakami, K., J. Taguchi, T. Murata, and R.K. Puri. 2001. The interleukin-13 receptor alpha2 chain: an essential component for binding and internalization but not for interleukin-13-induced signal transduction through the STAT6 pathway. *Blood.* 97:2673–2679.
29. von der Weid, T., M. Kopf, G. Kohler, and J. Langhorne. 1994. The immune response to Plasmodium chabaudi malaria in interleukin-4-deficient mice. *Eur. J. Immunol.* 24: 2285–2293.
30. Lai, Y.H., and T.R. Mosmann. 1999. Mouse IL-13 enhances antibody production in vivo and acts directly on B cells in vitro to increase survival and hence antibody production. *J. Immunol.* 162:78–87.
31. McKenzie, G.J., C.L. Emson, S.E. Bell, S. Anderson, P. Fallon, G. Zurawski, R. Murray, R. Grencis, and A.N. McKenzie. 1998. Impaired development of Th2 cells in IL-13-deficient mice. *Immunity.* 9:423–432.
32. Oswald, I.P., R.T. Gazzinelli, A. Sher, and S.L. James. 1992. IL-10 synergizes with IL-4 and transforming growth factor-beta to inhibit macrophage cytotoxic activity. *J. Immunol.* 148:3578–3582.
33. Takeda, K., M. Kamanaka, T. Tanaka, T. Kishimoto, and S. Akira. 1996. Impaired IL-13-mediated functions of macrophages in STAT6-deficient mice. *J. Immunol.* 157:3220–3222.
34. Sato, T.A., M.B. Widmer, F.D. Finkelman, H. Madani, C.A. Jacobs, K.H. Grabstein, and C.R. Maliszewski. 1993. Recombinant soluble murine IL-4 receptor can inhibit or enhance IgE responses in vivo. *J. Immunol.* 150:2717–2723.
35. Fernandez-Botran, R., and E.S. Vitetta. 1991. Evidence that natural murine soluble interleukin 4 receptors may act as transport proteins. *J. Exp. Med.* 174:673–681.
36. Chiaramonte, M.G., D.D. Donaldson, A.W. Cheever, and T.A. Wynn. 1999. An IL-13 inhibitor blocks the development of hepatic fibrosis during a T-helper type 2-dominated inflammatory response. *J. Clin. Invest.* 104:777–785.
37. Bost, K., R. Holton, T. Cain, and J. Clements. 1996. In vivo treatment with anti-interleukin-13 antibodies significantly reduces the humoral immune response against an oral immunogen in mice. *Immunology.* 87:633–641.
38. Chiaramonte, M.G., M. Mentink-Kane, B.A. Jacobson, A.W. Cheeves, M.J. Whitters, M.E.P. Goad, A. Wong, M. Collins, D.D. Donaldson, M.J. Gruby, et al. 2003. Regulation and function of the interleukin 13 receptor α 2 during T helper cell type 2–dominant immune response. *J. Exp. Med.* 197:687–701.